Official journal
of the Spanish Society
of Chemotherapy

Original

Revista Española de Quimioterapia
doi:10.37201/req/153.2021

Emilio Garcia-Moran[1]
Marta Hernández[2]
David Abad[2]
José M. Eiros[1]

Putative Secondary Structure at 5'UTR as a Potential Antiviral Target against SARS-CoV-2

[1]Centro Nacional de la Gripe. Microbiology Department, Faculty of Medicine, Valladolid, Spain
[2]Laboratory of Microbiology and Molecular Biology, Instituto Tecnologico Agrario de Castilla y Leon, Valladolid, Spain

Article history
Received:26 October 2021; Accepted: 20 November 2021; Published: 15 December 2021

ABSTRACT

SARS-CoV-2 is an enveloped positive-sense single-stranded RNA coronavirus that causes COVID-19, of which the current outbreak has resulted in a high number of cases and fatalities throughout the world, even vaccine doses are being administered. The aim of this work was to scan the SARS-CoV-2 genome in search for therapeutic targets. We found a sequence in the 5'UTR (NC_045512:74-130), consisting of a typical heptamer next to a structured region that may cause ribosomal frameshifting. The potential biological value of this region is relevant through its low similarity with other viruses, including coronaviruses related to SARS-CoV, and its high sequence conservation within multiple SARS-CoV-2 isolates. We have predicted the secondary structure of the region by means of different bioinformatic tools. We have suggested a most probable secondary structure to proceed with a 3D reconstruction of the structured segment. Finally, we carried out virtual docking on the 3D structure to look for a binding site and then for drug ligands from a database of lead compounds. Several molecules that could be probably administered as oral drugs show promising binding affinity within the structured region, and so it could be possible interfere its potential regulatory role.

Keywords: SARS-CoV-2; frameshifting; 5'UTR; pseudoknot; molecular docking.

Estructura secundaria en 5'UTR como diana antiviral contra el SARS-CoV-2

RESUMEN

El SARS-CoV-2 es un coronavirus de ARN monocatenario de sentido positivo envuelto que causa COVID-19, del cual el brote actual ha provocado una gran cantidad de casos y muertes en todo el mundo, incluso cuando se están administrando dosis de vacunas. En este trabajo hemos escaneado el genoma del SARS-CoV-2 en busca de dianas terapéuticas. Encontramos una secuencia en el 5'UTR (NC \ _045512: 74-130), que consiste en un heptámero típico junto a una región estructurada que puede causar cambios en la pauta de lectura. El valor biológico potencial de esta región es relevante debido a su baja similitud con otros virus, incluidos los coronavirus relacionados con el SARS-CoV, y su alta conservación de secuencia dentro de múltiples aislados de SARS-CoV-2. Hemos predicho la estructura secundaria de la región mediante diferentes herramientas bioinformáticas. Hemos sugerido una estructura secundaria más probable para así proceder al acoplamiento virtual en la estructura 3D para buscar un sitio de unión y luego ligandos de fármacos. Hemos encontrado varias moléculas que probablemente podrían administrarse como fármacos orales muestran una afinidad de unión prometedora dentro de la región estructurada, por lo que es posible que interfieran en su posible función reguladora de la replicación viral.

Palabras clave: SARS-CoV-2, cambios en la pauta de lectura, 5'UTR, pseudonudo, acoplamiento virtual

INTRODUCTION

On March 11th, the World Health Organization (WHO) declared COVID-19 a clinical pandemic (primarily pneumonia and gastroenteritis) caused by the SARS-CoV-2 virus. As of end October 2021 the pandemic outbreak has caused almost five million deaths worldwide, although almost 7 million peo-

Correspondence:
Emilio Garcia-Moran
Centro Nacional de la Gripe. Microbiology Department, Faculty of Medicine, 47005 Valladolid, Spain
E-mail: egarmo@egarmo.com

ple are vaccinated. SARS-CoV-2 belongs to the *Coronaviridae* family and is related to SARS-CoV and Middle East Respiratory Syndrome (MERS)-CoV (79% and 50% genomic similarity, respectively). SARS-CoV caused an epidemic outbreak in 2003 and MERS caused an outbreak in 2012 [1]. Those three viruses belong to the *Betacoronavirus* genus. Coronaviruses cause zoonotic infections, so they may spill over from a host species to a different one through small changes in their genome. SARS-CoV-2 demonstrated a high genetic similarity (more than 85%) to a virus group known as SARS related coronavirus (SARSr-CoV), which are isolated from animal hosts, including *Hipposideros* bats and pangolins (*Manis javanica*). These species seem to be candidates as intermediate hosts for SARS-CoV-2 [2,3].

These viruses have a positively translated single strand RNA genome and they use programmed –1 ribosomal frameshifting (–1 PRF) to direct the synthesis of immediate early proteins that prepare the infected cell for takeover by the virus. Frameshifting is a smart mechanism for the translation of a genomic sequence into two different proteins by moving the translation frame one position in the union between RNA and the ribosome [4]. A typical frameshifting signal has two essential elements: a characteristic heptanucleotide called the 'slippery' sequence, at which the ribosome-bound tRNAs slip into the -1 frame, and an adjacent mRNA secondary structure that stimulates this slippage process. The intermediate sequence between these two elements also has a typical size of less than twelve nucleotides. Often the secondary structure is more complex than a simple stem-loop between palindromic sequences, expanding into pseudoknots [5]. In terms of structure, a pseudoknot forms upon the base-pairing of a single-stranded region of RNA in the loop of a hairpin to a stretch of complementary nucleotides elsewhere in the RNA chain.

A set of bioinformatic tools has already been developed to predict these structures [6]. The mechanism of action of pseudoknots is not completely understood; some authors suggest that it appears to be linked to the helicase activity of the ribosome. When pseudoknots are located in coding regions, they modulate the elongation and termination steps of translation: the ribosome is able to switch from the zero reading frame to the –1 frame and translation continues in the new frame. When pseudoknots are in non-coding regions, they act on the regulation of the initiation of protein synthesis and on template recognition by the viral replicase guiding viral replication and packaging [7].

All coronaviruses have been reported to utilize programmed –1 ribosomal frameshifting to control the expression of their proteins. In 2005, Plant et al. [8] identified a three-stemmed mRNA pseudoknot inducing an efficient -1 ribosomal frameshift in the SARS-CoV genome. By this mechanism, the virus may produce a fusion protein that overlaps the regions ORF1a and ORF1b. This element encodes an ORF1ab polyprotein involved in ablating the host cellular innate immune response. Mutations affecting this structure decreased the rates of -1 PRF and had deleterious effects on the virus propagation. Recently, Kelly et al. [9] described the same pseudoknot in SARS-CoV-2, and they demonstrated frameshifting. This area is highly conserved between SARS-CoV and SARS-CoV-2, as there is only one single nucleotide difference, a C to A substitution at position 13,533 bp.

The frameshifting regions could be used as a target to fight viral infection [9]. Starting with early studies, point mutations at the slippery sequence have proved to have an important effect on viral replication [8]; thus, they can be also interesting points in the engineering of an attenuated virus for vaccine development. The inhibition of these regions by peptide antisense oligomers was studied by Neuman et al. [10]. After several passages in cell culture, virions escape the inhibition of replication but show attenuated forms. Rangan et al. [11], described highly structured areas of RNA that might be less accessible to complementary oligomers, but these convoluted areas would provide small binding sites for conventional drug molecules; therefore, a combination of scanning for structure and sequence conservation may be appropriate to find therapeutic targets. Previous studies using *in silico* methods found drug-like molecules that would inhibit SARS-CoV replication by action on the frameshifting region at the overlap between ORF1a and ORF1b [12]. The same molecule has been shown to affect replication in SARS-CoV-2 [9].

In this work, we scanned the SARS-CoV-2 genome to seek for novel likely critical areas for virus replication focusing on frameshifting predictors. We explored the likely biological relevance of this feature through the study of sequence conservation and its suitability as a potential drug target by the analysis of the structural properties and the drug docking prediction.

MATERIAL AND METHODS

Genomewide frameshifting signal search. A prediction of the relevant sequence and structures in the viral reference genome for SARS-CoV-2 (NC 045512) [13] was performed using the KnotInFrame tool [14]. The output determined the sequence and position of slippery sequences and nearby pseudoknots, since both criteria are needed to predict frameshifting. Our focus on a particular region was established by combining KnotInFrame output with biological knowledge. We focused on previously undescribed frameshifting regions and the likely regulatory roles of UTR regions. Once a sequence of interest met these criteria, an inspection of the predicted secondary structure was achieved with additional tools ipknot [15] and RNAfold from Vienna Suite [16]. The secondary structure for the segment of interest in dot bracket notation was chosen from the inspection of the overall conformation of the 5'UTR and assuring to include the slippery region. The likelihood of the secondary structure was assessed by computing the minimum free energy (MFE) of a large number of random sequences of SARS-CoV-2 of the same length as the sequence of interest into mFold, in order to obtain an empirical distribution of MFE and so assess how dominant the proposed structure would be [17].

Conservation of the sequence of interest. Sequence conservation was assessed for the sequence of interest deter-

mined in the previous step as a reliable trait of biological relevance. The conservation of the sequence of interest was evaluated in two steps. First, the conservation between SARS-CoV-2 and other human and animal hosted coronavirus genomes was studied by the computation of a cladogram and by the search for the alignment of the sequence of interest against a comprehensive viral database. A total of 21 high quality genomes from coronavirus hosted in humans and other species were selected based on subjective criteria regarding variability and relevant facts to build a cladogram. The genomes were downloaded from GenBank and aligned with Clustal Omega [18] using the default parameters. The cladogram was constructed using a maximum likelihood estimate with FastTree [19], under a GTT model of nucleotide evolution. The package ggtree [20] was used in R [21] to generate the graphic of the cladogram and the multiple sequence alignment (MSA). In addition to this alignment of the SARS-CoV-2 and another 20 coronavirus genomes, the sequence of interest was examined by ViroBLAST [22]. This tool provides a blastn [23] alignment with a comprehensive database of all types of virus, so that we would assess any casual homology with any other virus. Secondly, we evaluated the conservation of the sequence of interest within SARS-CoV-2 isolates from different geographic locations since the onset of the pandemic. We took advantage of the fast contribution of genomes into the GISAID database. We filtered the genomes in the database in order to retain only high quality records (length greater than 29,000 nt and with a low number of undetermined positions). The number of variant site strains was assessed by blastn [23], making the distinction of variants at the whole 5'UTR region (1-265 nucleotide positions); and the number of variants at the position of the sequence of interest. Further individual inspections of mismatched genomes were conducted to ensure whether the variation was not due to technical sequencing reasons.

Prediction of 3D structure and molecular docking. Upon consideration of different alternatives, the structure of the sequence of interest in dot-bracket notation and the underlying nucleotide sequence were imported into Rnacomposer [24] to obtain a 3D structure prediction in .pdb format. The file in .pdb format was used as input for the virtual scan for active sites. This task was carried out using Autodock tools suite [25]. This suite comprises the AutoGrid and Autoligand tools for the search of active sites in a molecular 3D structure. A combination of manual selection of the region of interest and automatic search space by the tools was used to obtain the coordinates and dimensions of a putative active site. These data were used as inputs for the molecular docking by the Autodock Vina tool. The virtual docking tested the binding of a set of molecules specially selected for drug screening: the NCBI maximum diversity set II. The affinity of molecules to bind the active site was assessed by the minimum free energy in Kcal/mol.

RESULTS

Frameshifting prediction. We used Knotinframe program [14] to detect cis-acting signals, the nucleotide sequence and the position of the heptameric slippery sites and near pseudoknots as prediction for –1 PRF. A list of genomic regions of SARS-CoV-2 (NC 045512.2) where a frameshifting signal was predicted by the KnotInFrame program is shown in Table 1. The stability of every predicted structure is also indicated by the MFE value, on the rightmost column. A more negative value of MFE represents a more stable and likely to be a functional structure. This value is mainly dependent on the length of the sequence. The pseudoknot we propose associated with the pattern sequence at position 76 (UUUAAAA) that was identified as –1 PRF, is ranked fourth and exhibit the lowest MFE

Table 1 **Summary of the output of KnotInFrame tool on NC_ 045512.2 genome.**

Slippery sequence	Slippery pos.	Pseudoknot start	Pseudoknot end	Length	Deltarel	MFE
TTTAAAC	13462	13469	13549	80	0.126	-34.80
GGGTTTA	4261	4268	4328	60	0.092	-15.60
AAATTTG	6071	6078	6158	80	0.076	-16.10
TTTAAAA[a]	76	83	123	40	0.070	-14.00
GGGTTTT	13348	13355	13475	120	0.051	-34.90
GGGTTTG	8183	8190	8270	80	0.049	-15.10
TTTAAAT	4264	4271	4331	60	0.047	-15.60
CCCAAAA	20646	20655	20773	120	0.046	-29.00
TTTAAAA	6514	6521	6621	100	0.038	-19.40
TTTAAAC	20817	20824	20924	100	0.035	-30.20
TTTTTTT	11076	11085	11183	100	0.035	-19.60

[a]The line in bold face was chosen as the sequence of interest. MFE: minimum free energy

```
70--------80--------90--------100-------110-------120-------130 bp position
CGAACUUUAAAAUCUGUGUGGCUGUCACUCGGCUGCAUGCUUAGUGCACUCAC
.........(((((((..((.((((.(((.....))).))))))..))))))        Rangan
.............(((((((((.....)))))))))((...[[)).... ]]        IPknot
...........(((((((((((...[[))))))(((.....]]))))....)))))).... IPknot-cutoff
.............(((((((((.....)))))))))((.....)).....          RnaFold
xxxxxxxxxxxx....[[[[[[[[.{{{{]]]]]]]].....}}}}.....x        KnotInFrame
```

Figure 1 | **Segment of 5'UTR NC 045512 sequence and different predicted secondary structures. The slippery heptamer is highlighted in yellow.**

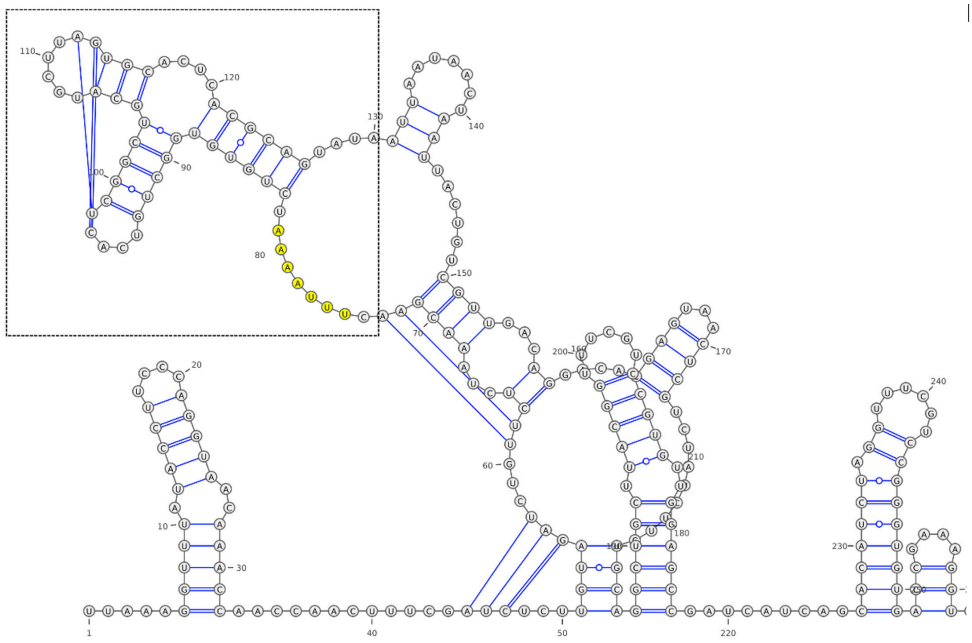

Figure 2 | **Secondary structure of 5'UTR region of NC 045512 as predicted by IPKnot. Region of interest framed on the top left. Slippery sequence in yellow.**

value among the predictions on the whole genome. However, all the other structured sequences are longer and this causes their stability not to be so much significantly higher than the region we propose associated with the slippery sequence located at position 76.

RNA 2D structure. The selected predicted frameshifting region clearly falls into the 5'UTR of NC_045512.2 reference genome [14], which spans from 1 to 265 nt as the first start codon for the coding sequence is at 266 position in SARS-CoV-2. However, if –1 PRF occurs within the 5'UTR region, probably at the U nucleotide at position 95 nt, then there is an upstream AUG codon at position 107 that can act as start codon and viral translation might be altered. The sequence of interest spanning from position 74:130 was selected and it is shown in Figure 1 along with the secondary structure as predicted by different programs in dot bracket notation. The IPknot tool [15] has been used in two fashions, firstly by the only input of the sequence of interest and secondly, by the input of the whole 5'UTR region, and then cutting out the prediction for positions 7:130. In both cases, IPknot predicts a knotted structure just downstream of the slippery region (the pattern of opening and closing brackets do not match, meaning that stem-loops bind to outer regions). Interestingly, the prediction we obtained using IPknot fully agrees with the prediction obtained recently in that genomic area using the Rosetta tool [11].

Similarly, the secondary structure of the whole 5'UTR regions was also obtained by IPknot tool and the graphical representation of that secondary structure using the VARNA software [26] is shown in Figure 2. Upon the inspection of the secondary structure, a sequence of interest spanning from position 74:130 was selected (left top corner) to include the

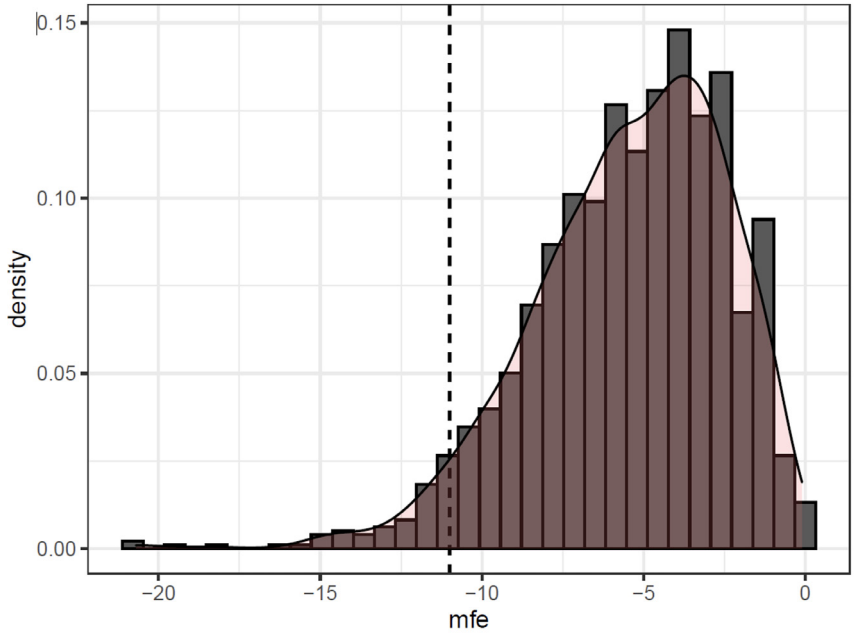

Figure 3 The histogram and density curve of the minimum free energy values of random sequences from NC 45512.2 of the same length as the sequence of interest. The vertical line at -11 Kcal/mol shows the computed MFE for the sequence of interest.

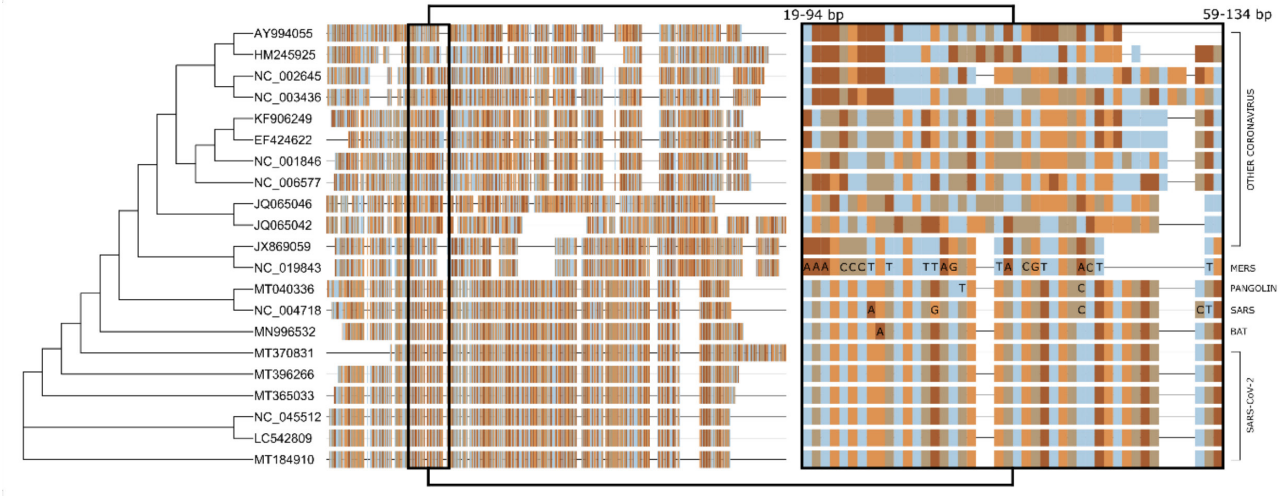

Figure 4 A cladogram and multiple sequence alignment. The middle part shows the alignment of the region in 21 coronaviruses. On the left, are shown the groups of sequences in terms of similarity. A zoomed in view on the region of the sequence of interest is shown on the right.

slippery sequence and neighbouring structured segment. The sequence (positions 74—130) was also used to proceed with the analysis so that it includes the slippery region and the structure of the stem and loop and the pseudoknot.

In order to test the probability of the predicted secondary structure as indicated by its computed MFE, we analyzed 1,509 random sequences from NC_45512.2 of the same length as the sequence of interest. Their MFE values were computed by mFold [17] to obtain an empirical distribution. The predicted value for the sequence of interest (-11 Kcal/mol) was ranked

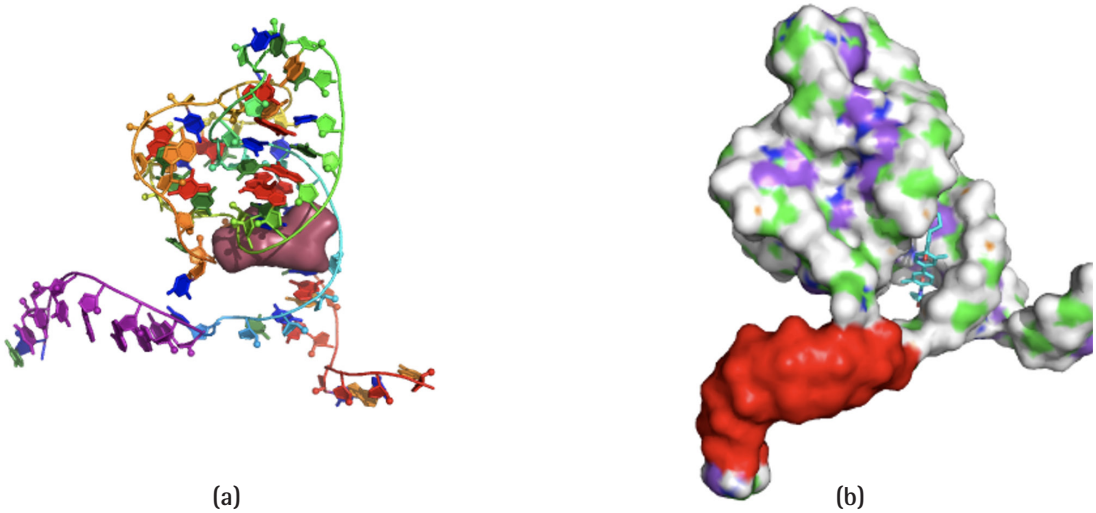

(a) (b)

Figure 5 (a) Graphical representation of the nucleotide backbone of the sequence of interest. The sequence of interest is shown from the 5' end (left) to the 3' end (right). The rounded purple volume in the middle shows the active site as predicted by the AutoDock suite tools. The slippery sequence is on the left bottom, in purple colour, the rest of nucleotide pieces are coded according to chemical composition. (b) Side view of the sequence of interest in a surface representation. The red area on the left shows the slippery sequence. The active ligand site holds one of the best matches: NSC308835/pubChem328761 (see Table 3) in its docked position.

Table 2 List of similar hits to NC 045512:74-130 in Viroblast database.

Host	GenBank accession no.	Date (year)	Score	Identities (Query length)	Percentage	Expect
Rhinolophus pusillus	JX993987.1	2011	86.0	52/55 (57)	95	1e-15
Rhinolophus sinicus	KJ473814.1	2013	86.0	53/57 (57)	93	1e-15
Rhinolophus sinicus	MG772933.1	2017	86.0	53/57 (57)	93	1e-15
Rhinolophus sinicus	MG772934.1	2017	86.0	53/57 (57)	93	1e-15
Mus musculus	HQ890526.1	2008	80.6	52/57 (57)	91	5e-14
Mus musculus	HQ890527.1	2008	80.6	52/57 (57)	91	5e-14
Mus musculus	HQ890528.1	2008	80.6	52/57 (57)	91	5e-14
Mus musculus	HQ890529.1	2008	80.6	52/57 (57)	91	5e-14
Mus musculus	HQ890530.1	2008	80.6	52/57 (57)	91	5e-14
Mus musculus	HQ890531.1	2008	80.6	52/57 (57)	91	5e-14

within empirical distribution of the MFE values. The histogram and frequency curve of this distribution is shown in Figure 3. The vertical line is set at -11 Kcal/mol. Clearly, few random sequences show this value. This value was at the top 5% of the negative endo of the distribution. This reveals that the predicted structure is fairly stable in relation to other segments of NC_45512, and supports that this sequence may occur in the predicted form of a stem-loop with outer bindings to form a pseudoknot and thus, along with the immediate slippery sequence form a frameshifting signal.

Genomic similarity. The conservation of the 74--130 region among *Coronaviridae* family is shown in Figure 4. Interestingly, while this region was identical in all the isolates from SARS-CoV-2 including isolates from human patients from distant geographical localizations (MT370831, New York; and

Table 3 Results of docking of lead compounds from NCI diversity set II against the predicted active site in the sequence of interest.

NSC id	pubChem id	MFE[a]	Molecular formula	H bond donors	H bond acceptors	Active torsions	Mol weight
293778	325266	-12.2	C40H26N4S	0	5	2	594.7
308835	328761	-11.1	C30H32N2O4	0	4	0	484.6
61610	247228	-11.1	C34H24N6O2	4	4	4	548.6
37641	235856	-11	C29H33FO6	2	7	4	496.6
319990	330740	-10.7	C23H18N6O2S2	4	6	4	474.6
93354	261360	-10.6	C28H33NO2S	1	4	1	447.6
122819	452548	-10.5	C32H32O23S	3	14	7	656.7
37553	235811	-10.5	C30H28N4O2	2	2	2	476.6
37641	235856	-10.5	C29H36FO6	2	7	4	496.6

[a]Values of predicted MFE in Kcal/mol. MFE: minimum free energy

LC542809, Japan) and from animals suspected to be infected from humans (MT396266, farm mink; and MT365033, zoo tiger), increasing differences were observed in other *Coronaviridae*. A minor difference in one nucleotide was found in a bat sequence (MT996532), while the differences increased in the pangolin hosted virus, and SARS-CoV-1 (NC_004718, Tor2 strain). Subsequently, we also tested the sequence of interest for similarity to other viruses on the Viroblast database [22]. The search parameters were kept at nominal values except for the word length, which was changed from ten to seven to increase the likelihood of matching slippery sequences. Viroblast search yielded 10 hits derived from two sources (Table 2): the top four hits were coronaviruses isolated in China from different species of bat *Rhinolophus pusillus/sinicus* between 2011 and 2017 and the latest hits a mouse-adapted laboratory model derived from SARS-CoV (consecutive GenBank accession numbers from HQ890526 to HQ890531.1; although these isolates were sampled from the Urbani strain GenBank AY278741 rather than Tor2). Finally, we evaluated the conservation of the sequence of interest among clinical SARS-CoV-2 isolates. The 5'UTR (1-265 nucleotide positions) of NC_045512.2 was searched using BLASTN [23] analysis against 54,466 high quality filtered genomes (out of 84,140) retrieved from GISAID on the 21st of August, 2020. While, only a 19,8% of the genomes (10,789 out of 54,466) had a 100\% identity in the complete 5'UTR, the 74—130 region was highly conserved, as it was 100\% identical in 99.3 % of SARS-CoV-2 genomes tested (53,077 out of 53,456).

RNA 3D structure. In order to carry out molecular docking on potential active sites of the sequence of interest was continued the nucleotide sequence in the Figure 1 and the selected region of the secondary structure in Figure 2 as inputs into RNAcomposer [24] to obtain a .pdb file of the nucleotide sequence. The results of the predicted 3D structure and the possible location of a drug binding site are shown in Figure 5. The volume of the binding site is the result of the exploration with Autodock tools. The coordinates of the binding site were obtained in .pdb format and they were passed into Autodock Vina (the exhaustiveness search parameter at a default value of eight; and the random seed sequence was fixed) [25]. The results of the docking by Autodock Vina against the lead compounds from the NCBI Maximum Diversity set II are shown in Table 3. The Autodock Vina predicted the affinity of the lead compounds by the computation of the MFE. As more negative values of MFE mean higher binding affinities, so the lead compounds were ranked by this value. The number of hydrogen bond donors and acceptors and the molecular weight in g/mol are annotation data from PubChem. These data show how likely a compound is to be used as an oral drug [27].

DISCUSSION

This study has revealed a previously unnoticed feature in the SARS-CoV-2 genome, which is likely to play a biological role on account of the remarkable conservation of its sequence and stability of the structure. The close occurrence of the slippery sequence and a likely stable pseudoknot suggests that this may be an area of frameshifting, in addition to the previously described overlapping region of ORF1a and ORF1b, where frameshifting has been proven for SARS-CoV [8] and also present in SARS-CoV-2 [9]. We focused on a different region, previously unnoticed in the 5'UTR. The fact that no protein may be linked with the sequence may argue against frameshifting, as may that of the overlap between ORF1a and ORF1b. Supporting the role of 5'UTR, Zhu et al. [28] demonstrated that different natural deletions in the 5'UTR of FMDV (foot-and-mouth disease virus) markedly affected the pathogenicity and species tropism of the virus. Frameshifting linked with 5'UTR has been described in HIV-1 [29], and in this case the structure next to the slippery sequence is a stem and loop, without additional pseudoknotting.

Another important endeavour of this work is to consider this RNA structured area as a useful target for feasible drug

intervention. Puzzlingly, the description of a possible drug against the pseudoknot involved in frameshifting between ORF1a and ORF1b in SARS-CoV did not progress to an actual drug for use in health care [12,30], probably due to the lag in time of this discovery after the 2003 SARS-CoV outbreak. The same molecule that was found to inhibit viral replication of SARS-CoV appears to be effective against SARS-CoV-2 [9].

Rangan et al. [11] performed a wide analysis on the SARS-CoV-2 and SARSr-CoV genomes, and they classified multiple regions in terms of the conservation and RNA structure. In agreement with our approach, they consider that structured regions would be ideal targets for small drug molecules. In Table 2 (eighth row) of their article, they describe, among others, sequence 40:157 of NC_045512-2 as highly conserved and structured. We reproduce in Figure 1 their proposal of structure for our region of interest. The result of the alignment of our sequence of interest against the Viroblast database showed that the sequence may have been close to SARS-CoV as described in 2003 [31]. We found two pathways of highly similar sequences; coronaviruses isolated from bats in the following years and from laboratory-derived strains developed to create a mouse-adapted model from the Urbani strain of SARS-CoV-2. Although outside of this work, these findings support the role of bats as intermediate hosts between SARS-CoV and SARS-CoV-2, and the possibility that some unrecognized variation in strains of SARS-CoV would manifest relevant features as with the sequence which we describe.

A limitation of our work is that it was restricted to computational analysis. This shortcoming is likely more relevant when it comes to the determination of the tridimensional structure of RNA and its subsequent docking. The determination of the crystal structure 3D prediction and drug docking has been developed for proteins rather than RNA. One of the features of RNA that makes docking difficult is its flexibility. However, successful discovery of ligands against SARS-Cov-2 pseudoknot by a computed 3D structure has been described before [12,30]. Clinical evidence of pharmacological actions against RNA viral genomes was achieved by drugs such as sofosbuvir (tradename Sovaldi) against Hepatitis C Virus (HCV). These drugs are described as nucleotide analogues. They bind to the target region as a complementary sequence would do but they differ from short chains of nucleotides so that they may resist lytic enzymes.

Our screening for drug ligands was an exploratory analysis, as it was limited to 1,507 compounds from NCBI maximum diversity set II. In Table 3 several compounds have a MFE lower than -10 Kcal/mol. This suggests that a search against a larger catalog would yield multiple candidates. Several compounds on the Table 3 can meet the criteria to be orally useful drugs according to Lipinski's rule of five [29]. We point out that the compound ranked second in terms of MFE affinity: NSC 308835 as it meets every Lipinski's criterion. The next best compound did not meet that molecular weight, which should be less than 500 g/mol, though by a small margin. This fact does not preclude oral activity. NSC61610 was given orally, once a day to mice in an experimental model of H1N1 influenza infection [32]. The mice had less mortality and the response was better than with tamiflu after the sixth day of infection. However, that mechanism of action is unrelated to interactions with viral RNA, as NSC61610 acts as a modulator of the immune response.

In conclusion, we have identified a relevant sequence in the 5'UTR region of SARS-CoV-2. It displays traits which have a high potential for playing an important role, either through frameshifting or other mechanism. A remarkable conservation within SARS-CoV-2 isolates strongly supports a biological role for this sequence. Our analysis of the drug susceptibility of this sequence is hindered by the inconsistent predictions of bioinformatic tools. It is however very likely that a strong structure of this area will allow effective action of relatively simple drug molecules.

ACKNOWLEDGMENTS

We kindly acknowledge Dr. Nigel Cook for English revision.

FUNDING

None to declare.

CONFLICT OF INTEREST

The authors declare no conflict of interest.

REFERENCES

1. Coleman CM, Frieman MB. Emergence of the Middle East Respiratory Syndrome coronavirus. PLoS pathogens. 2013;9:e1003595. doi: 10.1371/journal.ppat.1003595.
2. Wang H, Li X, Li T, Zhang S, Wang L, Wu X, Liu J. The genetic sequence, origin, and diagnosis of SARS-CoV-2. Eur. J. Clin. Microbiol. Infect. Dis. 2020; 39(9):1629-35. doi: 10.1007/s10096-020-03899-4.
3. Han GZ. Pangolins Harbor SARS-CoV-2-Related Coronaviruses. Trends Microbiol., 2020,28(7):515-17. doi: 10.1016/j.tim.2020.04.001.
4. Jacks T, Madhani HD, Masiarz FR, Varmus HE. Signals for ribosomal frameshifting in the Rous sarcoma virus gag-pol region. Cell. 1988;55(3):447-58. doi: 10.1016/0092-8674(88)90031-1.
5. Brierley I, Pennell S, Gilbert RJC. Viral RNA pseudoknots, versatile motifs in gene expression and replication. Nat Rev Microbiol. 2007;5(8):598-610. doi: 10.1038/nrmicro1704.
6. Lim CS, Brown CM. Know your enemy, Successful bioinformatics approaches to predict functional RNA structures in viral RNAs. Front Microbiol. 2018;4;8:2582. doi: 10.3389/fmicb.2017.02582.
7. Fehr AR, Perlman S. Coronaviruses, an overview of their replication and pathogenesis. Methods in molecular biology (Clifton, N.J.). 2015;1282:1-23. doi: 10.1007/978-1-4939-2438-7_1.
8. Plant EP, Perez-Alvarado GC, Jacobs JL, Mukhopadhyay B, Hennig

M, Dinman JD. A three-stemmed mRNA pseudoknot in the SARS coronavirus frameshift signal. PLOS Biology. 2005;3(6):e172. doi: 10.1371/journal.pbio.0030172.

9. Kelly JA, Olson AN, Neupane K, Munshi S, San Emeterio J, Pollack L, Woodside MT, Dinman JD. Structural and functional conservation of the programmed -1 ribosomal frameshift signal of SARS coronavirus 2 (SARS-CoV-2). J. Biol. Chem. 2020;31;295(31):10741-48. doi: 10.1074/jbc.AC120.013449.
10. Neuman BW, Stein DA, Kroeker AD, Churchill MJ, Kim AM, Kuhn P, Dawson P, Moulton HM, Bestwick RK, Iversen PL, Buchmeier MJ. Inhibition, escape, and attenuated growth of severe acute respiratory syndrome coronavirus treated with antisense morpholino oligomers. J. Virol. 2005;79(15):9665-76. doi: 10.1128/JVI.79.15.9665-9676.2005.
11. Rangan R, Zheludev IN, Das R. RNA genome conservation and secondary structure in SARS-CoV-2 and SARS-related viruses, a first look. RNA. 2020;26(8):937-59. doi: 10.1261/rna.076141.120.
12. Park H-J, Park S-J. Virtual Screening for RNA-Interacting Small Molecules. In: Dinman J. (eds) Biophysical approaches to translational control of gene expression. Biophysics for the Life Sciences, vol 1. Springer, New York, NY. 2012;1:235-52. doi:10.1007/978-1-4614-3991-2_12.
13. Wu F, Zhao S, Yu B, Chen Y-M, Wang W, Song Z-G, Hu Y, Tao Z-W, Tian J-H, Pei Y-Y, Yuan M-L, Zhang Y-L, Dai F-H, Liu Y, Wang Q-M, Zheng J-J, Xu L, Holmes EC, Zhang Y-Z. A new coronavirus associated with human respiratory disease in china. Nature. 2020;579(7798):265-69. doi: 10.1038/s41586-020-2008-3.
14. Theis C, Reeder J, Giegerich R. Knotinframe, prediction of -1 ribosomal frameshift events. Nucleic Acids Res. 2008;36(18):6013-20. doi: 10.1093/nar/gkn578.
15. Sato K, Kato Y, Hamada M, Akutsu T, Asai K. IPknot, fast and accurate prediction of RNA secondary structures with pseudoknots using integer programming. Bioinformatics. 2011;27(13):i85-93. doi: 10.1093/bioinformatics/btr215.
16. Lorenz R, Bernhart SH, zu Siederdissen HC, Tafer H, Flamm C, Stadler PF, Hofacker IL. ViennaRNA package 2.0. Algorithms for molecular biology. 2011; 6:26 doi: 10.1186/1748-7188-6-26.
17. Gruber AR, Lorenz R, Bernhart SH, Neubouck R, Hofacker IL. The Vienna RNA websuite. Nucleic Acids Res. 2008; 36(Web Server issue):W70-74. doi: 10.1093/nar/gkn188.
18. Sievers F, Wilm A, Dineen D, Gibson TJ, Karplus K, Li W, Lopez R, McWilliam H, Remmert M, Soding J, Thompson JD, Higgins DG. Fast, scalable generation of high-quality protein multiple sequence alignments using Clustal Omega. Mol Syst Biol. 2011;7:539. doi: 10.1038/msb.2011.75.
19. Price MN, Dehal, PS, Arkin AP. FastTree, computing large minimum evolution trees with profiles instead of a distance matrix. Mol Biol Evol. 2009;26(7):1641-50. doi: 10.1093/molbev/msp077.
20. Yu G. Using ggtree to visualize data on tree-like structures. Curr Protoc Bioinformatics. 2020;69(1):e96. doi: 10.1002/cpbi.96.
21. R Core Team. R, A Language and Environment for Statistical Computing. R Foundation for Statistical Computing, Vienna, Austria, 2017.
22. Deng W, Nickle DC, Learn GH, Maust B, Mullins JI. Viroblast, a standalone blast web server for flexible queries of multiple databases and user's datasets. Bioinformatics. 2007;23(17):2334-6. doi: 10.1093/bioinformatics/btm331.
23. Altschul SF, Gish W, Miller W, Myers EW, Lipman DJ. Basic local alignment search tool. J Mol Biol. 1990;215(3):403-10. doi: 10.1016/S0022-2836(05)80360-2.
24. Popenda M, Szachniuk M, Antczak M, Purzycka KJ, Lukasiak P, Bartol N, Blazewicz J, Adamiak RW. Automated 3D structure composition for large RNAs. Nucleic Acids Res. 2012;40(14),e112. doi: 10.1093/nar/gks339.
25. Trott O, Olson AJ. AutoDock Vina, improving the speed and accuracy of docking with a new scoring func tion, efficient optimization, and multithreading. J Comput Chem. 2010;31(2),455-61. doi: 10.1002/jcc.21334.
26. Darty K, Denise A, Ponty Y. VARNA, Interactive drawing and editing of the RNA secondary structure. Bioinformatics. 2009;25(15),1974-75. doi: 10.1093/bioinformatics/btp250.
27. Lipinski CA, Lombardo F, Dominy BW, Feeney PJ. Experimental and computational approaches to estimate solubility and permeability in drug discovery and development settings. Adv Drug Deliv Rev. 2001;46(1-3):3-26. doi: 10.1016/s0169-409x(00)00129-0.
28. Zhu Z, Yang F, Cao W, Liu H, Zhang K, Tian H, Dang W, He J, Guo J, Liu X, Zheng H. The pseudoknot region of the 5' untranslated region is a determinant of viral tropism and virulence of foot-and-mouth disease virus. J Virol. 2019;93(8):e02039-18. doi: 10.1128/JVI.02039-18.
29. Charbonneau J, Gendron K, Ferbeyre G, Brakier-Gingras L. The 5' UTR of HIV-1 full-length mRNA and the tat viral protein modulate the Programmed -1 ribosomal frameshift that generates HIV-1 enzymes. RNA. 2012;18(3):519-29. doi: 10.1261/rna.030346.111.
30. Park SJ, Kim YG, Park HJ. Identification of RNA pseudoknot-binding ligand that inhibits the -1 ribosomal frameshifting of SARS-coronavirus by structure-based virtual screening. J Am Chem Soc. 2011;133(26):10094-100. doi: 10.1021/ja1098325.
31. Roberts A, Deming D, Paddock C D, Cheng A, Yount B, Vogel L, Herman B D, Sheahan T, Heise M, Genrich G L, Zaki S R, Baric R, Subbarao K. A mouse-adapted SARS-coronavirus causes disease and mortality in balb/c mice. PLoS Pathog. 2007;3:e5. doi: 10.1371/journal.ppat.0030005.
32. Leber A, Bassaganya-Riera J, Tubau-Juni N, Zoccoli-Rodriguez V, Lu P, Godfrey V, Kale S, Hontecillas R. Lanthionine synthetase c-like 2 modulates immune responses to influenza virus infection. Front Immunol. 2017;8:178. doi: 10.3389/fimmu.2017.00178.